Korean J. Chem. Eng., 40(10), 2384-2395 (2023)
DOI: 10.1007/s11814-023-1492-1

pISSN: 0256-1115
eISSN: 1975-7220

ZIF-8 derived porous carbon/ZnO as an effective nanocomposite adsorbent for removal of acetic acid

Mohammadali Amidi and Ehsan Salehi†

Department of Chemical Engineering, Faculty of Engineering, Arak University, Arak 38156-8-8349, Iran
(*Received 18 February 2023 • Revised 22 April 2023 • Accepted 8 May 2023*)

Abstract−A porous carbon/zinc oxide nanocomposite adsorbent was prepared by carbonization/oxidation of ZIF8 metal-organic framework (MOF) and then used to investigate the adsorption of acetic acid from water. Preliminary tests revealed that the adsorbent composed of 25% porous carbon/zinc oxide and 75% zeolite could result in superior acetic acid removal. Response surface methodology and central composite design algorithm (CCD) were used to optimize the operating variables affecting the acid removal. The optimal conditions were obtained at the initial acid concentration of 257.5 mg/L, the adsorbent amount of 152.5 mg, the contact time of 32.5 min and the sample volume of 28.75 mL. In the optimal conditions, an adsorption capacity equal to 106 mg/g was obtained. The experimental equilibrium adsorption was well-described by the Langmuir isotherm model, reflecting the monolayer chemisorption of the acid on the active sites. In addition, adsorption on the developed adsorbent followed the pseudo-second-order kinetics, and according to the thermodynamic study results, the adsorption was exothermic and spontaneous. In conclusion, the adsorption capacity of the porous carbon/zinc oxide-zeolite composite was fair, while its removal rate was extremely higher compared to that of the similar adsorbents.

Keywords: Acetic Acid, Adsorption, Metal Organic Frameworks, Porous Carbon, Zeolite

INTRODUCTION

With the increasing progress of industry and technology, the amount of environmental pollution, especially water resources, has increased in the same proportion [1]. Many efforts have been made in various fields to reduce the menace of the environmental pollution that threatens the biosphere, animals, plants and humans [2]. Therefore, removing pollutants from water sources, or, in other words, water purification, is a very important issue. In the meantime, with the ever-increasing expansion of parent industries such as oil, gas and petrochemicals, due to the large volume of water demand in these large industries, the existence of water and wastewater treatment units to reuse industrial wastewater and process water (water used in the processes) and to minimize wastewater discharge has become an inevitable necessity. Water pollutants are divided into organic and inorganic categories [3]. Removing organic pollutants is much more difficult and is also more important because of their greater toxicity [4]. Although organic pollutants are diverse and nowadays a special method is recommended to remove each type of them in the industry, in the meantime, the removal of organic acids, especially acetic acid and formic acid has received increasing attention. These acids are among the most abundant carboxylic acids which are available in process water and wastewater of petrochemical industries and refineries [5]. The concentration of these two organic acids has been reported to be higher than other organic acids in the effluents of petrochemical industries [6]. The presence of acetic and formic acids in drinking water causes problems such as kidney stones, nausea and general weakness of the body [7]. In terms of the purification process, the presence of organic pollutants in the water disrupts the biological purification of wastewater, which is usually used in water purification units of petrochemical industries and refineries [8]. Acetic acid is a typical representative of organic acids in an effluent, to attain the discharge standards of effluent, the removal of acetic acid by the adsorption process is necessary. To date, various adsorbents have been developed and used for acetic acid adsorption. For the effluents, the total organic carbon (TOC) value must be lower than 5,000 mg/L, and the acetic acid concentration should be lower than 1 wt%. Generally, the lower the acid concentration in the effluent, the more difficult it is to adsorb. Therefore, it is important to explore an adsorbent with excellent adsorption capacity as well as fast kinetic rate for acetic acid removal from the effluents containing low concentrations of acetic acid (ranging from 100 to 1,000 ppm). The goal of the removal of acetic acid and formic acid from process water in the petrochemical industry is to find an effective and economical method, as well as a practical purification strategy with high efficiency and effectiveness [9]. The concentration of these acids in industrial effluents is low but does not meet the standards required for disposal. There are different methods for removing organic pollutants from process water, which include different physical and chemical processes such as ion exchange [10], membrane filtration [11], electrodialysis [12], evaporative seepage [13], adsorption [14], precipitation [15] and catalytic and photocatalytic processes [16-18]. Usually, adsorption methods have been favored over other alternative methods due to affordable operating costs, high separation efficiency and proper controllability of the process [19].

†To whom correspondence should be addressed.
E-mail: e-salehi@araku.ac.ir

Adekola and her colleagues used activated carbon made from the oil seeds of the shea tree, which is native to central African countries, to remove acetic acid and formic acid from an aqueous solution [7]. In another study, Narin investigated the adsorption of acetic acid from aqueous solutions on a type of zeolite [20].

In this research, the aim is to adsorb acetic acid from aqueous media. Therefore, adding metal oxides and combining them in a suitable way to the carbon base provides a good adsorbent for acetic acid. The decomposition of organic acids on metal oxide surfaces is usually defined based on acid-base reactions. In the case of acid adsorption, the acidic proton is separated by the negative oxygen anions and the remaining anion reacts with the reactive cationic sites of the surface [21]. To modify the surface of activated carbon and zeolite, metal oxides should be appropriately distributed on these substrates in the form of nanoparticles; otherwise, the proper surface modification is not usually done and it is possible that the pores of the substrates be filled and the specific surface area is accordingly decreased. On the other hand, due to the acidity of the environment, nanoparticles should have good stability on the substrate. Therefore, in this research, for the first time, a porous carbon structure provided by uniform dispersion of metal nanoparticles on its surface was fabricated by in-situ synthesis method inside the structure of metal-organic frameworks (MOF). By applying this method, the accumulation of nanoparticles is prohibited and controlled. Accordingly, the filling of the porous carbon cavities can be appropriately avoided. Carbonization and oxidation at high-temperature help to activate the structure. Adding zeolite to MOF adsorbent helps to reduce costs and provides the conditions for industrialization of these adsorbents. The general aim of this research is to make a surface-modified adsorbent based on porous carbon (PC), metal oxide nanoparticles derived from ZIF 8 and zeolite. Processing ZIF-8 using template materials results in creation of a new class of composite materials that combines the advantages of both precursors [22-24]. The use of heat-treated ZIF8 to produce zinc oxide (ZnO) and PC with zeolite composition as an effective adsorbent to remove acetic acid from the water was investigated in the current study. The CCD method was used to achieve optimal adsorption conditions. Isotherms, kinetics and thermodynamics of adsorption were also assessed in optimal adsorption conditions.

EXPERIMENTAL

1. Materials and Instrumentation

Acetic acid (glacial), sodium hydroxide (99%), phenolphthalein (indicator), ethanol (absolute), zinc nitrate hexahydrate (for synthesis), 2-Methylimidazole (Hmim), ammonium hydroxide (25-30%), acetonitrile and phosphoric acid were purchased from Merck (Germany). Zeolite molecular sieve (ZSM5) was purchased from Dr. Mojallali Commpany (Iran). Distilled deionized water was used for the preparation of aqueous solutions. A Waters Alliance (1525, Waters Milford, MA, USA) HPLC equipped with a Rheodyne injector and a PDA (model 996) was utilized for the determination of acetic acid concentration. The target analyte was separated by a C18 column (25 mm×4.6 mm, 5 μm particle size) held at 35 °C. A mixture of acetonitrile and 50 mM phosphate buffer at pH=3 (2 : 98, v/v) was delivered at a flow rate of 1 mL min^{-1} as the mobile phase in an isocratic elution mode. FESEM images were obtained by SIGMA VP field emission scanning electron microscope (FESEM) FEI NOVA NanoSEM450 instrument. X-ray diffraction (XRD) patterns were recorded by a Philips-X'pertpro diffractometer containing Ni-filtered Cu Ka radiation. A Perkin Elmer, Spectrum GX Furrier transforms infrared (FTIR) was also used for more characterization.

2. Green Synthesis of ZIF8

ZIF8 was synthesized through a straightforward way within a short time. 0.594 g of zinc nitrate hexahydrate (2 mmol) was dissolved in 3 ml of deionized water. 0.328 g of Hmim (4 mmol) was dissolved in 3.76 g of ammonium hydroxide solution (64 mmol of NH_3). Then, zinc nitrate and 2-methylimidazole solutions were mixed. The final solution had a molar composition of Zn : Hmim : NH_3 : H_2O 1 : 2 : 32 : 157. The solution quickly turned into a milky suspension and then was stirred for 10 minutes at room temperature (25 °C), until crystallization was completed. The resultant precipitate was collected by centrifugation and washed with deionized water three times until the pH of the final product was equal to 7, then it was dried at 60 °C overnight [25].

3. Carbonization/Oxidation of ZIF8 and Mixing with Zeolite

The prepared ZIF-8 was calcined in a tubular furnace with a heating rate of 3 °C/min and heated at 500 °C for 2 h under nitrogen atmosphere, and then heated to room temperature at a rate of 10 °C/min. The powder was slowly cooled to obtain a carbonized structure such that its volatiles were removed. Then, the carbonized ZIF8 was oxidized under air atmosphere with a heating rate of 10 °C/min and kept at a the temperature of 250 °C for 1 h. Next, N_2 gas was purged for 10 min and finally cooled slowly [26]. The resultant composite was PC/ZnO that ZnO nanoparticles uniformly distributed on the PC surface.

To prepare the PC/ZnO/zeolite composites, different mass ratios of carbon-to- zinc oxide were provided by mixing of different proportions of ZIF8 with the powdered ZSM zeolite (i.e., ZIF8 : ZSM equal to 1 : 1, 1 : 2, 1 : 3, and 3 : 1). The prepared precursors were completely mixed using a mill. Milling continued until a homogenized powder was obtained.

4. Experimental Design for Removal of Acetic Acid

To optimize the effective variables in the batch adsorption, the central composite design (CCD) algorithm of the response surface methodology (RSM) was employed. According to the preliminary tests, four influencing factors, including the amount of adsorbent, acid concentration, the volume of the aqueous solution, and the removal time, were considered as the main effective variables and the acid removal percentage as the response. Based on CCD design, 26 tests for 4 factors in 5 levels were proposed by the Design Expert software. The conditions of the proposed tests are presented in Table 1. Two solutions were prepared in the same concentration of each run. Then, one of the solutions was titrated with 0.1 or 0.01 M, depending on the acid concentration. The other solution with corresponding test conditions according to the parameters of Table 1 was stirred, and after the completion of the removal time, it was filtered and the amount of acetic acid in the filtered solution was determined by titration with sodium hydroxide in the presence of phenolphthalein indicator. The amount of acid removal was calculated from the difference in acid concentration before and after the

removal process.

RESULTS AND DISCUSSION

1. Characterization

The SEM images of ZIF-8 nanoparticles are given in Fig. 1A. As can be seen, these nanostructures are very small polyhedral nanoparticles that are slightly agglomerated. In Fig. 1C, the SEM images of zeolite can be seen, which are placed next to each other in the form of regular strings, and due to their very good morphology they can be used as a very good sorbent platform. When the ZIF-8 nanoparticles were placed in a furnace containing nitrogen at a temperature of 500 °C, the transformation of its organic ligand into PC occurred and the resultant nanoparticles were regular. By oxidation of the structure under air atmosphere, ZnO nanoparticles were also created in the structure. Also, the SEM images of the PC/ZnO-ZSM5 composite can be seen in Fig. 1D, the microstructure images show that the PC/ZnO nanoparticles are dispersed on the surface of the zeolite rods. It shows successful synthesis of this nanocomposite adsorbent (Fig. 1).

The XRD patterns related to the synthesized sorbents including ZIF-8, Zn-PC, ZnO-PC and Zeolite-ZnO-PC are depicted in Fig. 2. The XRD pattern shows the presence of a crystalline phase in the synthesized structure. ZIF-8 peaks at angles of 10.35, 12.75, 16.40, 18.6 and 20.1 are related to plates (002), (112), (013), (222) and (123), respectively. After pyrolysis of ZIF-8, the product remains in the zinc oxide phase. In addition, the XRD pattern of ZnO shows mild diffraction peaks in ZnO/porous carbon, which may be due to the graphitization of organic groups and a low amount of ZnO [27]. In the XRD pattern of PC/Zn, the peaks in the angles of 32.1, 35.4, 37.8, 48.2 and 57.3 can be represented as crystal planes (100),

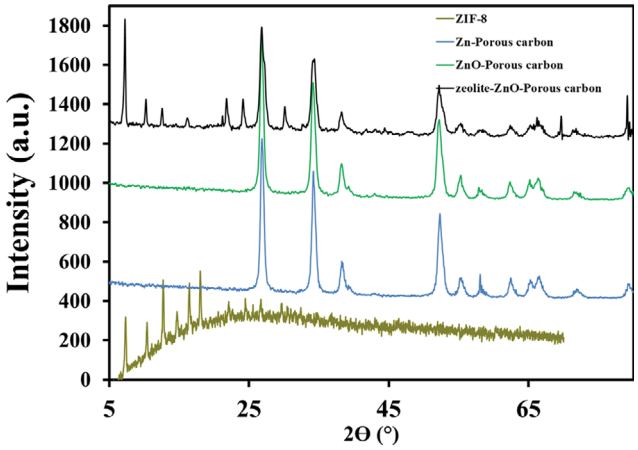

Fig. 2. XRD patterns of synthesized adsorbents.

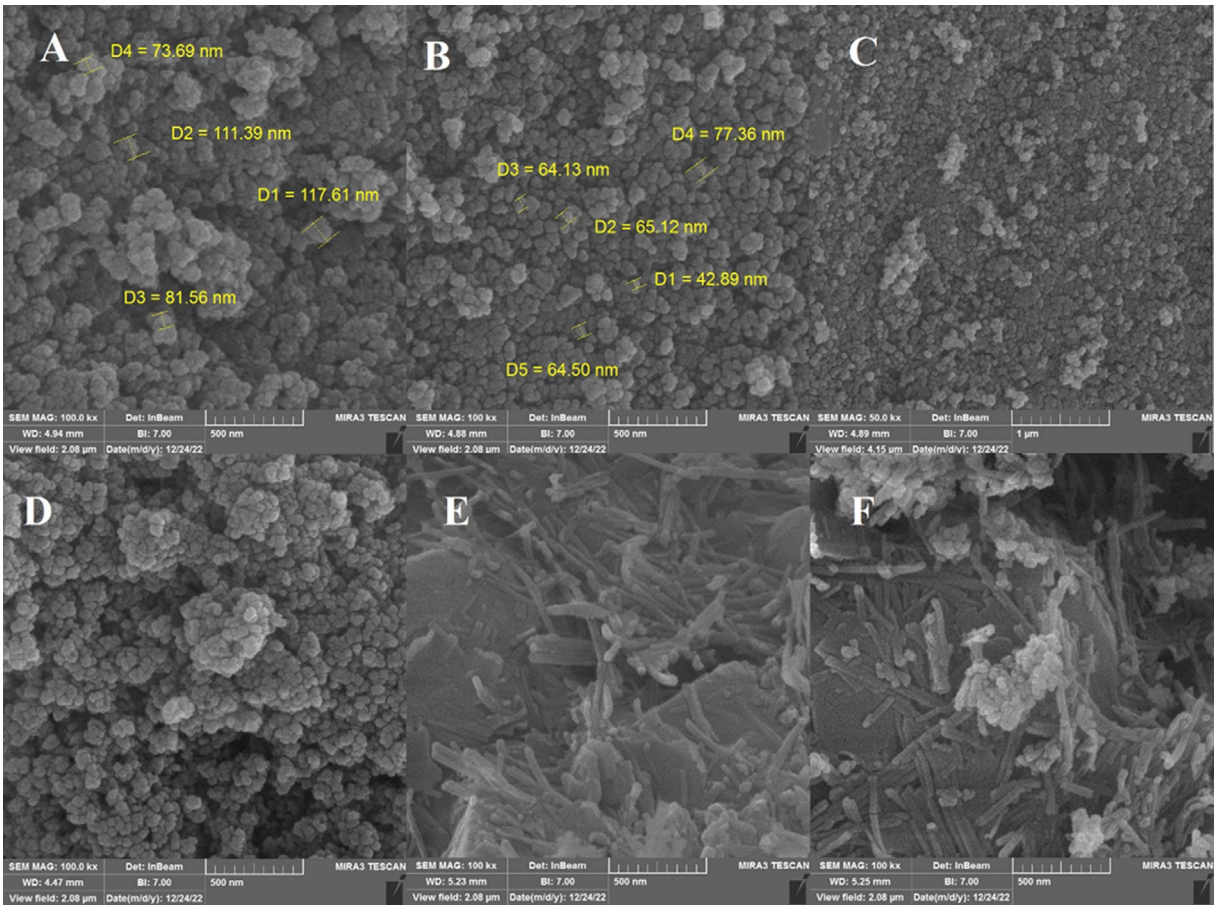

Fig. 1. SEM images of (A) ZIF8, (B, C) PC/Zn, (D) PC/ZnO, (E) zeolite and (F) composite of PC/ZnO-ZSM5.

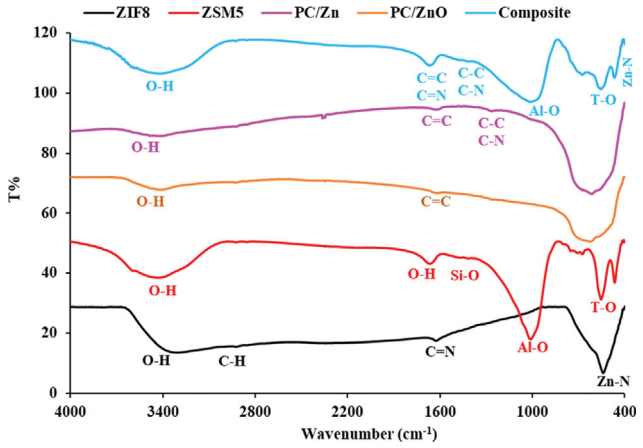

Fig. 3. FTIR spectrum of sorbents.

(002), (101), (102) and (110), while the peaks in the angles of 63.0, 66.1, 67.0, 69.1 and 77.0 are related to the crystal planes (103), (200), (112), (201), and (202), respectively. In the XRD pattern of Zeolite-ZnO-PC nanocomposite, there is a sum of diffraction peaks related to Zeolite and ZnO-PC nanoparticles, which indicates the successful synthesis of this composite.

To understand more about the structure of the Zeolite, ZIF-8, Zn-PC, ZnO-PC and Zeolite-ZnO-PC, FT-IR analysis was performed (Fig. 3). In the FTIR spectrum of the zeolite, a sharp peak is observed at 1,015 cm^{-1}, which is related to asymmetric stretching vibrations (Al-O). Another peak is observed at 674 cm^{-1}, which is related to the internal vibrations of the T-O symmetric stretching type. Two peaks of 1,671 cm^{-1} and 3,432 cm^{-1} are related to the presence of water molecules in the zeolite structure; the first peak is related to the bending vibration of the water molecule and the second one is related to the symmetric stretching vibration of the hydroxyl water molecule attached to the oxygen of the framework. Finally, the narrow and intense band at 1,465 cm^{-1} corresponds to the bending vibration of Si-O. The FTIR spectrum of ZIF-8 shows the peaks at 3,325 and 2,915 cm^{-1} are, respectively, related to C-H stretching vibrations of the aliphatic and aromatic imidazole rings. The peak located at 1,610 cm^{-1} is related to C=N stretching vibrations. The tiny peaks located at 600-1,500 cm^{-1} are related to the bending and stretching vibrations of the ring, and the peak located at 500 cm^{-1} belongs to the Zn-N vibration. The Zn/PC obtained from the carbonization of ZIF-8 under a nitrogen atmosphere shows a small peak at 1,230 cm^{-1} which can be attributed to C-C, C-N stretching. The peak at 1,617 cm^{-1} may be related to C=C of the aromatic ring and C=N in N-doped carbon (Fig. 3).

2. Optimization of Adsorbent Composition

To investigate the effect of the adsorbent composition on the removal of acetic acid, different adsorbents with different composition of porous carbon/zinc oxide obtained from ZIF8 and zeolite were prepared and analyzed. Fig. 4(a) shows the changes related to the amount of acid removal versus carbon-to-ZnO composition of the adsorbents. As can be seen, the combination of components has a synergistic effect, and in the combination of 50-50 mass ration of porous carbon/zinc oxide obtained from ZIF8 and zeolite, the highest removal efficiency was obtained. To more accurately investigate the impact of the composite composition on acid adsorption, different ZIF8/zeolite ratios of 0 : 100, 75 : 25, 50 : 50, 25 : 75, and 0 : 100 were mixed and investigated. It was observed that composite containing 25% porous carbon/zinc oxide (obtained from ZIF8) and 75% zeolite could tabulate the highest removal efficiency value (Fig. 4(b)), and so, it was used for further optimization experiments.

The exploitation of the high surface area-to-volume ratios of zinc oxide nanoparticles is specifically aimed while improving the overall performance of the composite. Porous carbon is one of the best sorbents due to its microporous structure and high specific surface area. Zeolites are microporous crystalline alumino-silicates, composed of TO4 tetrahedra (T=Si or Al) with tetrahedral configuration of neighboring oxygen atoms. Their unique properties are attributed to their alumino-silicate surfaces which serve as active sites for chemical reactions and a cage structure used as clathrate for molecular entrapment.

3. Investigating the Removal Ability of Developed Nonabsorbent for Acetic Acid

To investigate the effect of different parameters on the adsorption, the experimental design method and the central composite design (CCD) model were used. In this method, the designed conditions of each run are determined with the help of the suggested table of the experiments. Then, the modeling was done, and using

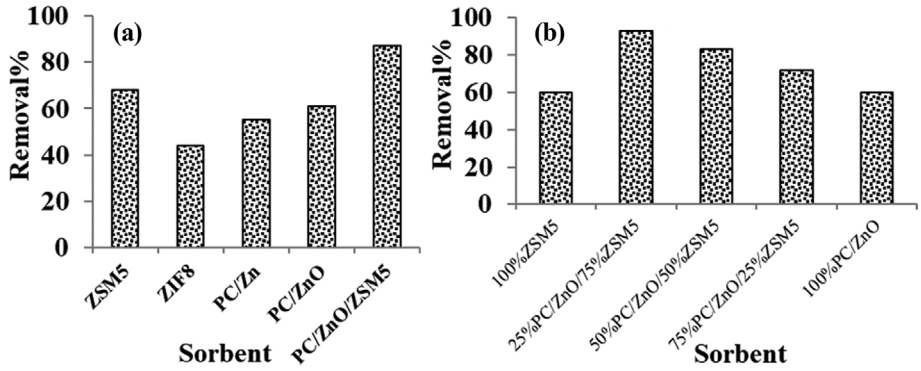

Fig. 4. Comparison of the efficiency of different composite in removing acetic acid, (a) Pure and 50 : 50 mass ratio mix of precursor components, (b) Composites with different precursors compositions.

Table 1. Experimental design and result of acetic acid removal

Run	A: sorbent amount (mg)	B: Acid concentration (ppm)	C: Time (min)	Sample volume (mL)	Removal%
1	57.5	752.5	32.5	76.25	35.6
2	105	505	55	100	52.7
3	152.5	752.5	77.5	28.75	78.8
4	105	505	10	52.5	60.0
5	105	505	55	52.5	54.0
6	57.5	752.5	77.5	76.25	28.3
7	57.5	752.5	77.5	28.75	63.2
8	152.5	257.5	77.5	28.75	86.7
9	105	1,000	55	52.5	26.0
10	105	505	100	52.5	62.3
11	152.5	257.5	32.5	76.25	71.4
12	10	505	55	52.5	25.9
13	152.5	752.5	77.5	76.25	42.9
14	152.5	257.5	77.5	76.25	63.3
15	105	505	55	5	90.0
16	152.5	752.5	32.5	28.75	78.6
17	57.5	257.5	32.5	28.75	53.8
18	57.5	752.5	32.5	28.75	48.3
19	57.5	257.5	77.5	28.75	64.3
20	57.5	257.5	77.5	76.25	35.5
21	152.5	257.5	32.5	28.75	80.0
22	200	505	55	52.5	78.2
23	105	505	55	52.5	60.4
24	57.5	257.5	32.5	76.25	55.2
25	152.5	752.5	32.5	76.25	51.7
26	105	10	55	52.5	80.0

Table 2. ANOVA analysis

Source	Sum of squares	df	Mean square	F-value	P-value	
Model	6,801.64	4	1,700.41	41.91	<0.0001	Significant
A-Sorbent amount	2,808.84	1	2,808.84	69.23	<0.0001	
B-Acid concentration	671.70	1	671.70	16.56	0.0008	
C-Adsorption time	1.08	1	1.08	0.0266	0.8723	
D-Sample solution volume	3,002.80	1	3,002.80	74.01	<0.0001	
Residual	689.70	17	40.57			
Lack of fit	669.37	16	41.84	2.06	0.5043	Not significant
Pure error	20.34	1	20.34			

the statistical methods of analysis of variance and p-value test, the effect of different parameters was determined. Also, the ability of the model to predict was analyzed by analyzing the accommodation of the model-predicted results with the experimental results. The results related to the design of the experiment and the removal of acetic acid on the PC/ZnO-zeolite composite can be seen in Table 1.

The statistical analysis of the model was done using the analysis of variance and the results are shown in Table 2. The p-value is less than 0.05, which indicates that the model is meaningful and can well predict the experimental conditions. The p-value for factors that is less than 0.05 means the response changes are significant. The linear equation obtained from the model is as follows:

$$\text{Removal } \% = 58.68 + 11.48\,A - 6.18\,B - 0.2251\,C - 12.98\,D$$

After calculating the model coefficients, the accuracy of the model should be evaluated. For this purpose, four criteria including the model significance test, model accuracy test, determination of R^2 and R_{adj}^2 coefficients, and analysis of residuals were used. Considering that the correlation coefficient of the model is higher than 0.9, it shows that the model is well capable of predicting various parameters and removal efficiency. Also, the accuracy adequacy parameter is a measure of the signal-to-noise ratio, and values higher than 4 indicate that the analysis signals have the necessary inten-

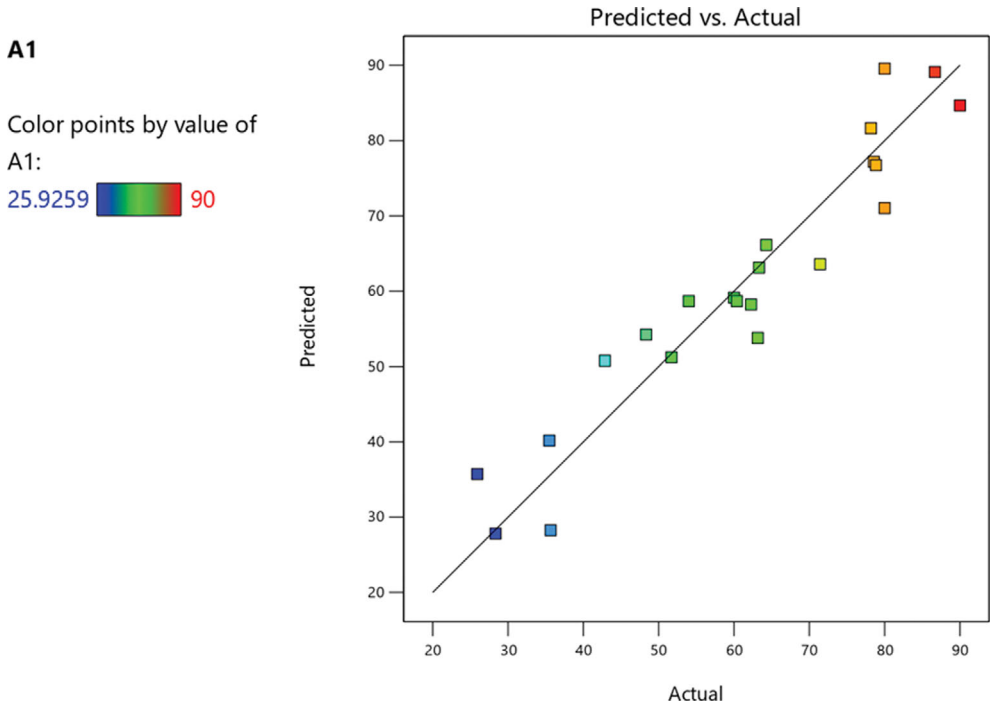

Fig. 5. Correlation curve between the predicted values and the actual values of removal efficiency by the proposed RSM model.

sity compared to the noise for model construction and prediction Fig. 5. Also, to validate the proposed model, the method of comparison between the predicted response and the actual values was done. Using the obtained graphs, it can be seen that there is a slight difference between the predicted data and the experimental data, and the obtained points are sufficiently close to the straight line, which indicates the appropriateness of the model.

4. Investigating the Effect of Effective Factors on the Amount of Acetic Acid Adsorption Using the RSM-based Model

In the present research work, to study the effective and efficient

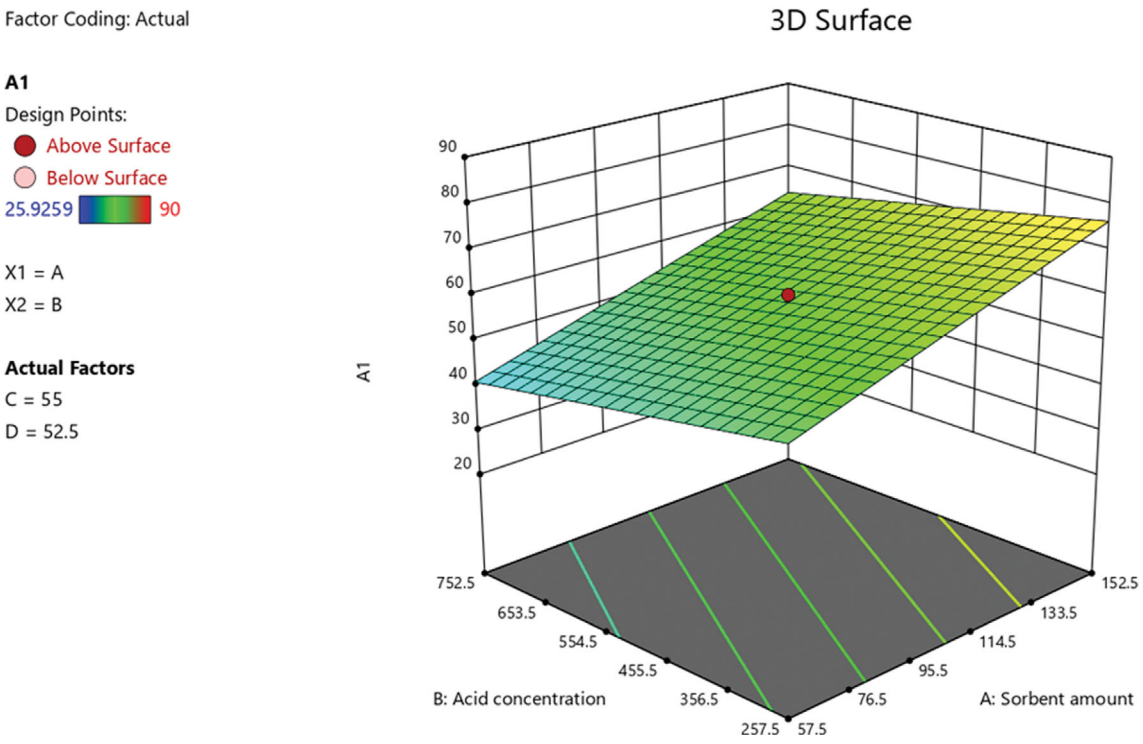

Fig. 6. RSM of the effect of adsorbent amount and acetic acid concentration on removal efficiency.

effects of binary interactions on acetic acid removal with the proposed method, the three-dimensional surface curves of the removal percentage of acid against two independent variables in the constant values of the third and fourth variables were plotted. As can be seen, the presence of an almost smooth surface without curvature in the response surface curves indicates the dominant effects of the linear and first-order interactions.

Determining the mutual interaction between the variables of the sorbent amount and acid concentration was achieved by changing two parameters and keeping the third and fourth parameters

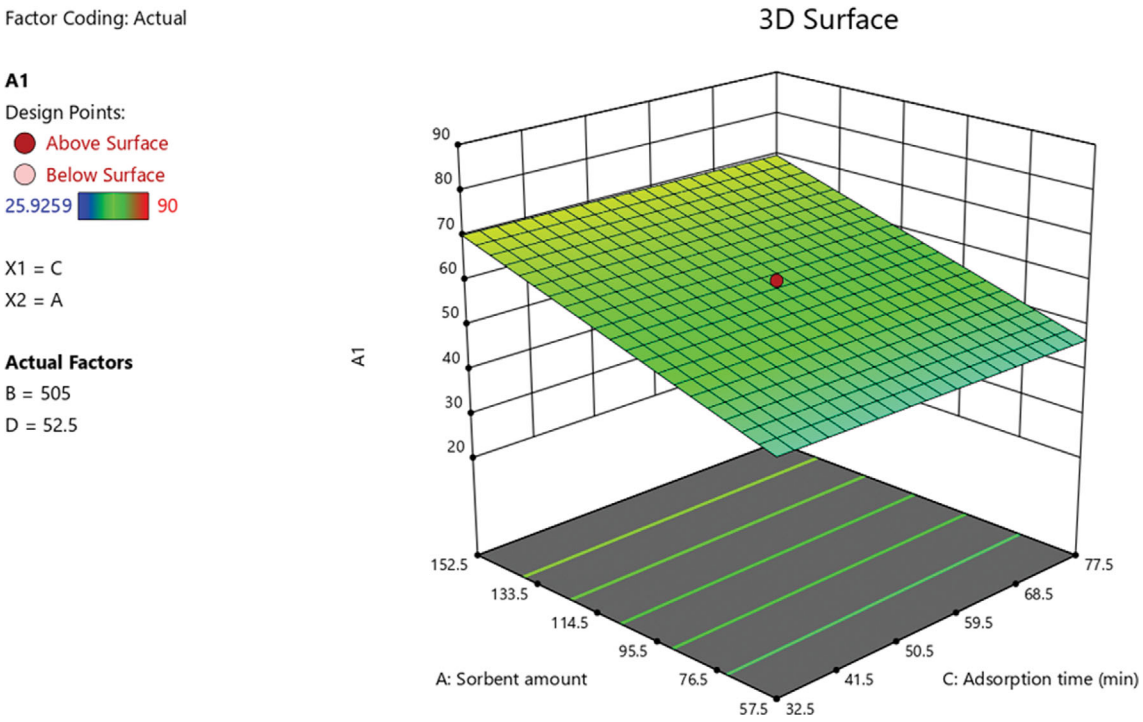

Fig. 7. RSM of the effect of adsorbent amount and adsorption time on removal efficiency.

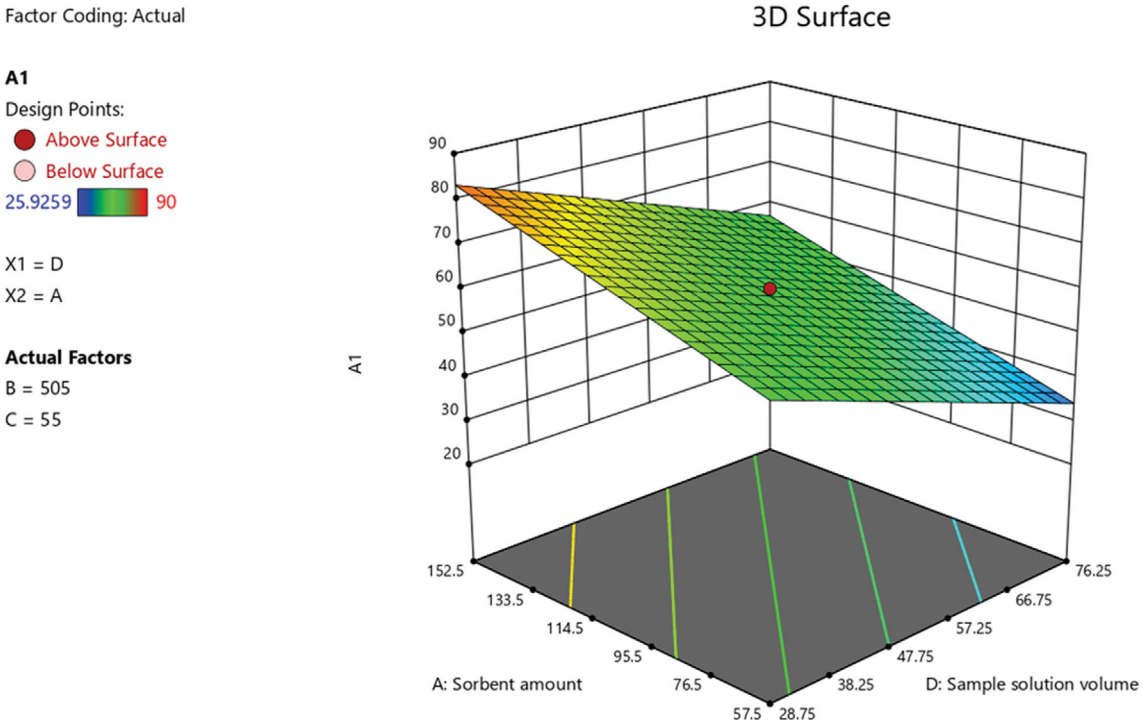

Fig. 8. RSM of the effect of adsorbent amount and sample volume on removal efficiency.

constant. Fig. 6 shows the simultaneous effect of changes in the amount of adsorbent and acid concentration on the efficiency of acetic acid removal. According to the shape, with an increasing amount of adsorbent and decreasing acid concentration, removal efficiency increases. It can also be seen that the reduction rate of removal is more affected by changes in the amount of adsorbent. It is clear that to remove more acid, a greater amount of sorbent is needed, and this results in increasing the removal efficiency. But, on the other hand, with the increase in the concentration of acid, the amount of sorbent becomes insufficient for this amount of acid and the efficiency decreases.

The mutual interaction between the variables of the adsorbent amount and adsorption time was investigated by changing two parameters and keeping the third and fourth parameters constant. Fig. 7 shows the simultaneous effect of changes in the amount of adsorbent and adsorption time on the efficiency of acetic acid removal. According to the shape, the amount of removal increases with the increase of time and amount of adsorbent.

The mutual interaction between the variables of adsorbent value and sample volume was investigated by changing two parameters and keeping the third and fourth parameters constant. Fig. 8 shows the simultaneous effect of the changes of these two factors on the efficiency of acetic acid removal. According to the figure, the amount of removal increases with an increasing amount of adsorbent and decreasing sample volume.

The final goal of the design of the experiment and presenting the model is to obtain the optimal values of the experimental conditions in which the removal efficiency is at the highest possible value. The obtained results can be influenced by the mutual effects between the parameters in addition to the independent effects. The response surface diagrams show the effects of the variables involved and the interaction between the two variables on the effectiveness of the experimental method in a state where other independent variables are kept constant at their central point. The response surface method is one of the appropriate options for evaluating the simultaneous effects of parameters and provides the possibility of spatial visualization of the predicted equation. The use of the response level curve provides us with important information about the binary interactions of the independent variables, such that their significance has been confirmed with the help of the variance analysis. The optimal conditions are summarized in Table 3.

5. Optimizing the Responses by Using the Utility Function

The utility function can be used to determine the optimal values according to an experimental design. In this function, the tuning value varies from zero to one, the criterion is one, and as the utility function gets closer to one, the possibility that the calculated

Table 3. The predicted optimal conditions by the model

Number	Sorbent amount	Acid concentration	Adsorption time	Sample solution volume	A1	Desirability	
1	152.500	257.500	32.500	28.750	89.543	0.993	Selected

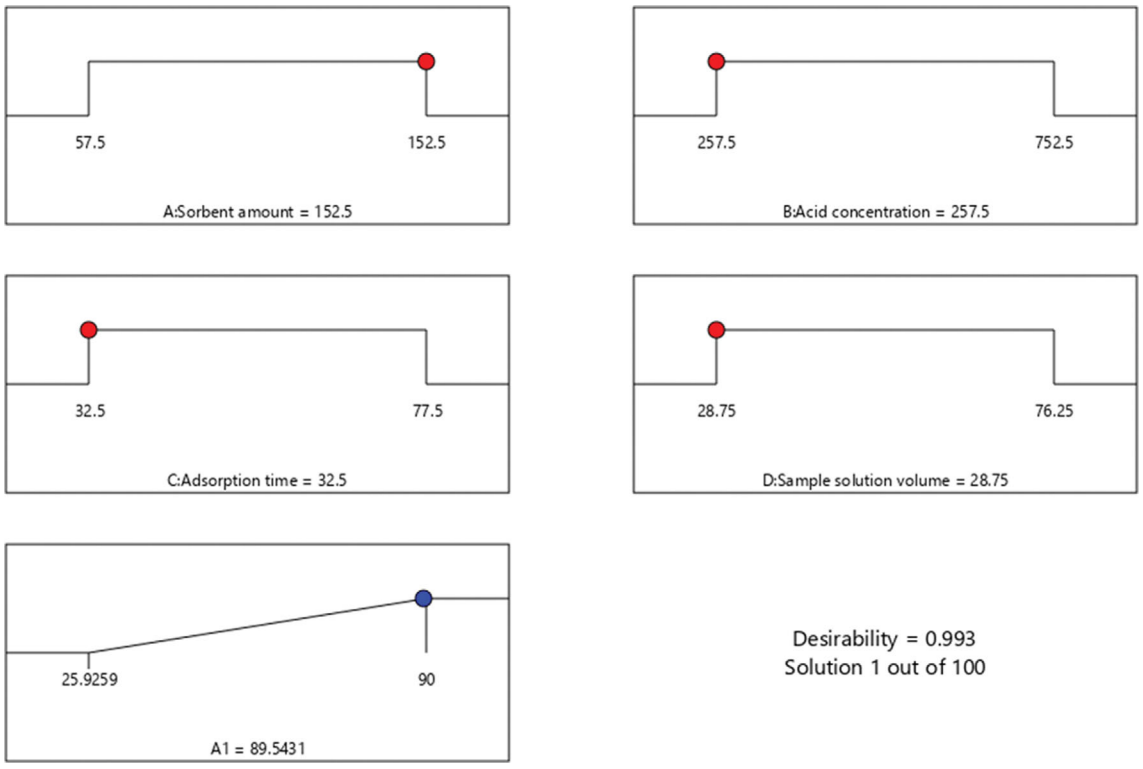

Fig. 9. Schematic of the optimal conditions for the adsorption of acetic acid using the utility function.

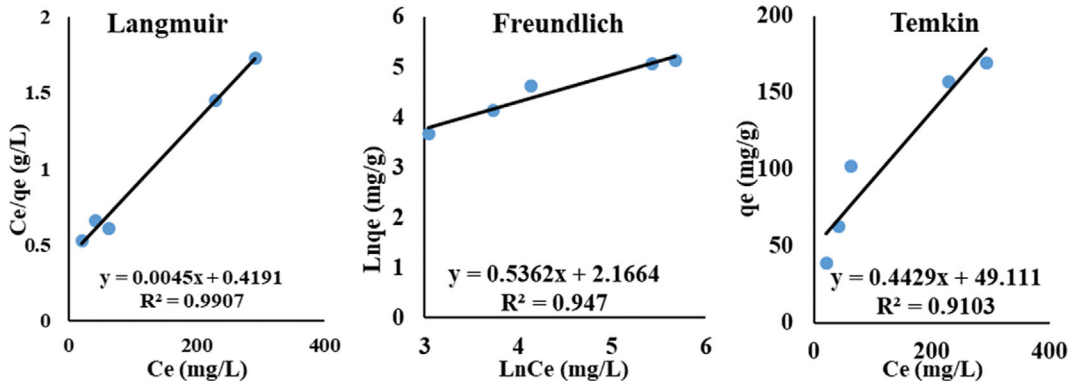

Fig. 10. Linear graphs of isotherms.

Table 4. Longmuir isotherm linear equation and calculated parameters value

Model	Parameters			
	Equation	q_m (mg g^{-1})	K_L (L mg^{-1})	R^2
Langmuir	$\frac{C_e}{q_e}=\frac{1}{q_m}C_e+\frac{1}{K_L q_m}$	222.22	0.0019	0.9907

point is the optimal point increases. Fig. 9 shows the optimal conditions resulting from the utility function analysis. The value of 0.993 for the utility function shows that the obtained optimal values are close to the actual optimal values. This indicates the usefulness of the proposed model.

6. Adsorption Isotherms

After determining the optimal adsorption conditions, it was found that the highest removal percentage could be obtained in the 152.25 mg amount of composite sorbent (PC/ZnO-zeolite), sample volume of 28.75 mL, initial acid concentration of 257.5 ppm and contact time equal to 32.5 min. Therefore, under these optimal conditions, isotherm, kinetic and thermodynamic studies were carried out.

The adsorption isotherm is a basic concept in the surface adsorption process. Isotherm is an equilibrium relationship between the amount of substance that is adsorbed and the concentration of this substance at a constant temperature. Based on literature, there are several models to describe laboratory data in the form of adsorption isotherms; the two-parameter isotherms of Freundlich, Langmuir and Temkin and the three-parameter isotherms of Dubinin-Radushkevich and Toth are more common models applied. By using the obtained adsorption data, information can be obtained about the mechanism, surface characteristics, and affinity of the adsorbate to the sorbent. Adsorption isotherms are very useful for understanding the type of adsorbent interaction, especially for the removal of organic compounds (Fig. 10). After drawing different equilibrium adsorption graphs by considering their correlation coefficient (R^2), it is possible to understand the type of equation governing the adsorption equilibria and measure the information related to the adsorption process, such as the relevant constant and the adsorption capacity of any adsorbent (q).

The mechanism of acid adsorption on the developed sorbent follows the Langmuir isotherm, which indicates the uniformity of the adsorbent surface and the maximum amount that can be adsorbed in the form of a single layer on the surface adsorbing material, so that all adsorption sites are of the same strength and acid adsorption occurred on a homogeneous surface. There is almost no lateral interaction among the adsorbed molecules. This model shows mainly chemical surface adsorption. The constants of the Langmuir model is presented in Table 4.

7. Study of Adsorption Kinetics

Adsorption kinetic investigation is very important because it can provide us with useful information about the adsorption mechanisms and, also, the time required for the equilibrium. Most prevalent kinetic models, first- and second-order kinetic models, intraparticle penetration and Elovich, were investigated to describe the adsorption kinetic and calculate the sorption rate constants. The information obtained for the adsorption of acetic acid according to the correlation coefficients as well as matching the adsorption

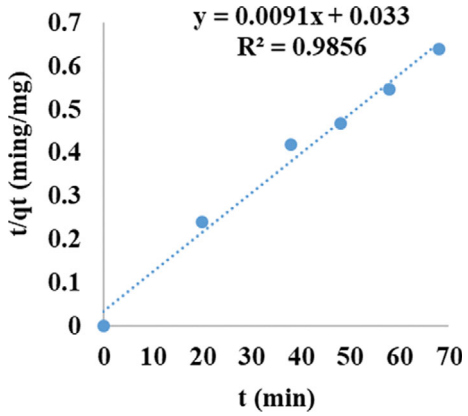

Fig. 11. The pseudo-second-order kinetic model for acetic acid adsorption on the PC/ZnO-zeolite.

Table 5. Calculated kinetic parameters for adsorption of acetic acid on PC/ZnO-zeolite based on a pseudo-second-order model

		Parameters		
Model	Equation	q_e (mg g^{-1})	k_2 (g mg^{-1} min^{-1})	R^2
Pseudo-second-order	$t/q_t=1/k_2q_e^2+t/q_e$	109.9	0.0025	0.9856

data with those predicted by the kinetic model showed that the adsorption on the developed adsorbent follows the pseudo-second-order kinetics (Fig. 11, Table 5). This means a good affinity between the acid molecules and the adsorption sites with a superior uptake rate.

8. Study of Adsorption Thermodynamic

Since adsorption is an equilibrium process, the maximum amount of analyte is adsorbed at the equilibrium time. To investigate the effect of temperature on the adsorption equilibria, the temperature was studied in the range of 10 to 58 °C. To calculate the important thermodynamic functions of adsorption (ΔS: entropy, ΔH: enthalpy, ΔG: Gibbs energy), the adsorption tests at several temperatures were carefully done. The van't Hoff equation is the relationship between the thermodynamic functions:

$$\Delta G^o = -RT\ln K_{(T)}$$

$$\ln K_{(T)} = -\frac{\Delta H^o}{R}\left(\frac{1}{T}\right) + \frac{\Delta S^o}{R}$$

$$\Delta G^o_{ad} = \Delta H^o_{ad} - T\Delta S^o_{ad}$$

The slope of plotting lnK(T) in terms of (1/T) is equal to $-\Delta H^o/R$ and its intercept value is equal to $\Delta S^o/R$. Fig. 12 shows the diagram related to the van't Hoff equation for the adsorption of acetic acid adsorption by the developed adsorbent. Thermodynamic parameters are reported in Table 6. According to the results presented in the table, the negative increase of Gibbs free energy with temperature indicates the spontaneity of the adsorption. Also, the negative values of ΔS^o indicate the reduction of the amount of irregularity during the adsorption process. In short, the values of thermodynamic parameters obtained show a spontaneous and exothermic process with a decrease in disorder for the studied adsorption.

9. HPLC-DAD Versus Titration Method for Acetic Acid Concentration Detection

The titration method was used to detect the acid acetic concentration only due to its simplicity and no need for specific instruments. We also repeated some experiments in optimal conditions

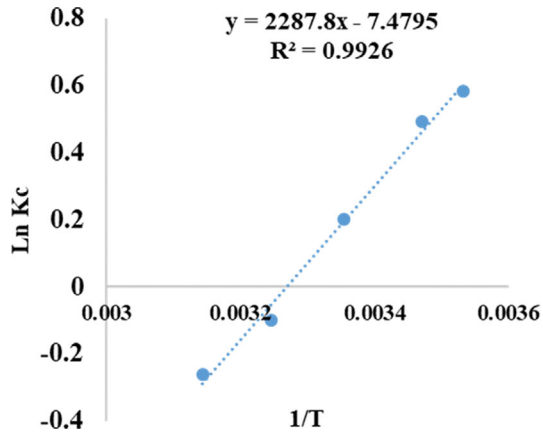

Fig. 12. Thermodynamic diagram of van't Hoff equation

Table 6. Values of thermodynamic parameters

ΔS^o (J mol^{-1} K^{-1})	ΔH^o (kJ mol^{-1})	ΔG^o (kJ mol^{-1})	T (K)
−62.18	−19.02	−1.72	278.15
		−1.41	283.15
		−1.10	288.15
		−0.48	298.15
		+0.14	308.15
		+0.76	318.15

with HPLC-DAD (Fig. 13), to check the accuracy of the titration method. The results of the two methods were compared by the statistical t-test as presented in Table 7. The t-test results clearly show that there is a good agreement between the results obtained by the two methods (by a confidence level of around 95%). The calculated t values in all concentrations are smaller than the $t_{critical}$ (1.895), reflecting the desirability of both of the methods.

10. Comparison with Similar Adsorbents

The removal of acetic acid on the different adsorbents was compared and the corresponding results are summarized in Table 8. It

Table 7. Comparing acetic acid removal results by titration and HPLC-DAD methods

Target	C_0 (ppm)	Removal%		*t* statistical test	p (*t*-value)
		Titration	HPLC-DAD		
Acetic acide	50	98.1	98.9	0.058	0.851
	150	91.6	90.2		
	257	93.1	92.5		
	375	81.8	79.8		
	605	72.5	68.9		
	1,000	70.1	70.0		

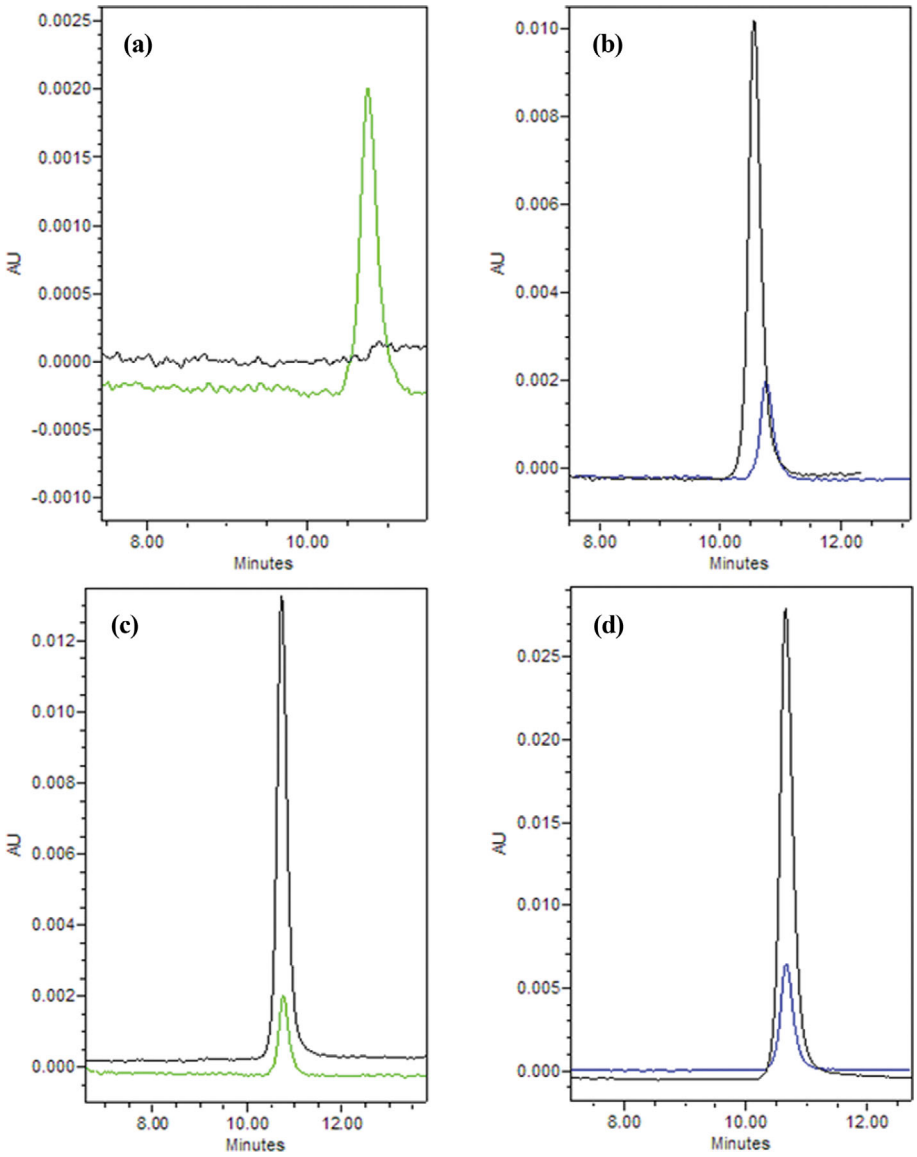

Fig. 13. HPLC-DAD chromatograms of acetic acid solution before and after removal by the developed sorbent ((a) 50, (b) 257, (c) 375 and (d) 605 ppm acetic acid).

Table 8. Comparison of the developed adsorbents with other acetic acid-adsorbents

Sorbent	Acid concentration range (ppm)	Sorbent amount (mg)	Adsorption equilibrium time (min)	Isotherm	Capacity (mg/g)	References
UiO-66	988-3,0400	100	360	Freundlich	270.2	[28]
Zeolite 13X	12,000-71,900	5,000	360	Freundlich	383	[29]
Flyash activated carbon	600-6,000	1,000	30	Langmuir	71.56	[30]
PC/ZnO/zeolite	100-1,000	152.5	32.5	Langmuir	106	This study

can be seen that the adsorption capacity of the developed sorbent for acetic acid is larger than that of the activated carbon, which might be attributed to the strong interaction between acetic acid and Zn and also the high surface area of zeolite and porous carbon. The results indicated that has a good capacity to remove acetic acid from water. In comparison to other methods for synthesizing adsorbents, the developed method for synthesizing PC/ZnO/zeolite is faster and easier. Moreover, in comparison with UiO66, PC/ZnO/zeolite has a more facile, affordable and fast synthesizing procedure. In addition, PC/ZnO/zeolite and activated carbon show much faster kinetic (shorter equilibrium time), compared to the other adsorbents. In conclusion, the adsorption capacity of the developed sorbent is fair, while, its removal rate is extremely higher compared to those of the similar adsorbents. Adsorption kinetic rate is an

important criterion for adsorption process industrialization. Size of the equipment reduces with decreasing the adsorption equilibrium time.

CONCLUSIONS

The adsorption of acetic acid was studied on PC/ZnO obtained by carbonization/oxidation of ZIF-8 as a zeolite nanocomposite. The design of the experiment was employed to optimize the parameters affecting the acid removal. The importance and significance of the proposed model as well as its accuracy in predicting the results were evaluated by ANOVA. The importance and significance of the quadratic model were evaluated with the four criteria of Fisher's ratio test (F test), model accuracy test (LOF), R^2 and R^2 (Adj.) coefficients, as well as the residual analysis. There is a good fit between the experimental data and the data-based model. Optimal adsorption conditions were obtained as the initial acid concentration of 257.5 mg/L, the adsorbent amount of 152.5 mg, the contact time of 32.5 min and the sample volume of 28.75 mL. Under optimal conditions, isotherm, thermodynamic and kinetic studies were investigated. The adsorption of acetic acid on the developed adsorbent followed the Langmuir isotherm model, which means that it is most likely monolayer chemisorption. The adsorption kinetic had a good fit with the pseudo-second-order equation, and finally, the thermodynamic study results indicated spontaneity, exothermicity, and entropy reduction of the system during the adsorption. Generally, it was concluded that the proposed adsorbent showed acceptable adsorption capacity together with an extremely high uptake rate for acetic acid removal from water.

ACKNOWLEDGEMENTS

The authors express their appreciation for the support of Arak University during completion of this work.

CONFLICT OF INTEREST DECLARATION

The authors deny any financial and personal conflict of interest that could have affected the present work.

REFERENCES

1. Y. Zhang, M. Sun, R. Yang, X. Li, L. Zhang and M. Li, *Ecol. Indic.*, **122**, 107314 (2021).
2. P. Saremi, *IJAEB*, **5**, 252 (2020).
3. L. Liang, F. Xi, W. Tan, X. Meng, B. Hu and X. Wang, *BCR*, **3**, 3 (2021).
4. Z. Aksu, *Process Biochem.*, **40**, 3 (2005).
5. S. Kumar and B. Babu, *Separation of carboxylic acids from waste water via reactive extraction*, International Convention on Water Resources Development and Management (ICWRDM), Pilani, India, Citeseer (2008).
6. V. Gandhi, M. Mishra and P. A. Joshi, *Mater. Sci. Forum*, **712**, 175 (2012).
7. F. A. Adekola and I. A. Oba, *Appl. Water Sci.*, **7**, 6 (2017).
8. M. Jain, A. Majumder, P. S. Ghosal and A. K. Gupta, *J. Environ. Manage.*, **272**, 111057 (2020).
9. K. D. Patil and B. D. Kulkarni, *J. Water Pollut. Purif. Res.*, **1**, 2 (2014).
10. V. K. Gupta, I. Ali, T. A. Saleh, A. Nayak and S. Agarwal, *Rsc Adv.*, **2**, 16 (2012).
11. F. E. Titchou, H. Zazou, H. Afanga, J. El Gaayda, R. A. Akbour, P. V. Nidheesh and M. Hamdani, *Chem. Eng. Process*, **169**, 108631 (2021).
12. H. Tian, Y. Wang, Y. Pei and J. C. Crittenden, *Appl. Energy*, **262**, 114482 (2020).
13. M. Minella, V. Maurino, C. Minero and D. Vione, *Int. J. Environ. Anal. Chem.*, **93**, 15 (2013).
14. M. N. Rashed, Organic Pollutants-Monitoring, Risk and Treatment, Intech, 7 (2013).
15. E. L. Foletto, W. R. B. d. Santos, S. L. Jahn, M. M. Bassaco, M. A. Mazutti, A. Cancelier and A. Gündel, *Desalin. Water Treat.*, **51**, 13 (2013).
16. F. S. Freyria, M. Armandi, M. Compagnoni, G. Ramis, I. Rossetti and B. Bonelli, *J. Nanosci. Nanotechnol.*, **17**, 6 (2017).
17. V. Wankhade Atul, G. Gaikwad, M. Dhonde, N. Khaty and S. Thakare, *Res. J. Chem. Environ.*, **17**, 84 (2013).
18. W. Zhao, M. Adeel, P. Zhang, P. Zhou, L. Huang, Y. Zhao, M. A. Ahmad, N. Shakoor, B. Lou and Y. Jiang, *Environ. Sci. Nano*, **9**, 1 (2022).
19. B. M. Travália and M. B. Soares Forte, *J. Chem. Eng. Data*, **65**, 9 (2020).
20. G. Narin and J. Turk. *Chem. Soc. Sect. B: Chem. Eng.*, **1**, 2 (2017).
21. O. Gamba, H. Noei, J. i. Pavelec, R. Bliem, M. Schmid, U. Diebold, A. Stierle and G. S. Parkinson, *J. Phys. Chem. C*, **119**, 35 (2015).
22. H. N. Abdelhamid, D. Georgouvelas, U. Edlund and A. P. Mathew, *J. Chem. Eng.*, **446**, 136614 (2022).
23. A. I. Soliman, A.-M. A. Abdel-Wahab and H. N. Abdelhamid, *RSC Adv.*, **12**, 12 (2022).
24. H. N. Abdelhamid, S. A. Al Kiey and W. Sharmoukh, *Appl. Organomet. Chem.*, **36**, 1 (2022).
25. M. He, J. Yao, Q. Liu, K. Wang, F. Chen and H. Wang, *Micropor. Mesopor. Mater.*, **184**, 55 (2014).
26. S.-L. Jian, Y.-J. Huang, M.-H. Yeh and K.-C. Ho, *J. Mater. Chem. A*, **6**, 12 (2018).
27. L. Wang, X. Zhu, Y. Guan, J. Zhang, F. Ai, W. Zhang, Y. Xiang, S. Vijayan, G. Li and Y. Huang, *Energy Storage Mater.*, **11**, 2104 (2018).
28. H. Zhang, X. Lan, P. Bai and X. Guo, *Chem. Eng. Res. Des.*, **111**, 127 (2016).
29. H. Zhang, Y. Wang, P. Bai, X. Guo and X. Ni, *J. Chem. Eng. Data*, **61**, 1 (2016).
30. N. Kannan and A. Xavier, *Toxicol. Environ. Chem.*, **79**, 1 (2001).